Bull Eng Geol Environ
DOI 10.1007/s10064-016-0947-6

ORIGINAL PAPER

Estimation of the joint roughness coefficient (JRC) of rock joints by vector similarity measures

Rui Yong[1] · Jun Ye[1] · Qi-Feng Liang[1] · Man Huang[1] · Shi-Gui Du[1]

Received: 17 June 2016 / Accepted: 23 September 2016

Abstract Accurate determination of joint roughness coefficient (JRC) of rock joints is essential for evaluating the influence of surface roughness on the shear behavior of rock joints. The JRC values of rock joints are typically measured by visual comparison against Barton's standard JRC profiles. However, its accuracy is strongly affected by personal bias. In the present study, a new comparison method is proposed for JRC evaluation to overcome the drawback of conventional visual comparison methods based on vector similarity measures (VSMs). The feature vectors are obtained by analyzing the angular variation of line segments of both standard JRC profiles and test profiles obtained from three kinds of natural rocks with a sampling interval of 0.5 mm. The roughness similarity degrees between test profiles and standard profiles are evaluated by the Jaccard, Dice, and cosine similarity measures. The JRC values of the test profiles are then determined according to the maximum relation index based on the similarity degrees. In the present study, a comparative analysis between the VSMs method and the JRC evaluation method using different roughness parameters demonstrated that the VSMs method is effective and accurate for JRC measurement.

Keywords Rock joint · Joint roughness coefficient (JRC) · Roughness amplitude · Vector similarity measure

✉ Shi-Gui Du
dushigui@126.com

[1] Key Laboratory of Rock Mechanics and Geohazards, Shaoxing University, Shaoxing 312000, People's Republic of China

Introduction

It has long been recognized that rock joints play an important role regarding mechanical properties and deformation behavior of rock masses (Du et al. 2000; Andrade and Saraiva 2008; Yong et al. 2013; Özvan et al. 2014; Chen et al. 2016). Generally, the shear resistance depends on the frictional resistance and geometric irregularities along rock joint surfaces, in which the irregularity or roughness of rock joints is the hardest quantity to estimate (Du 1999; Tang et al. 2016). In addition, joint surface roughness has a significant impact on groundwater flow and solute migration (e.g. Zimmerman and Bodvarsson 1996; Boutt et al. 2006; Zhao et al. 2014). Over the past five decades, various empirical methods (e.g. Barton and Choubey 1977; Barton 1984; Du et al. 2009), statistical methods (e.g. Maerz et al. 1990; Tatone and Grasselli 2010; Zhang et al. 2014), and fractal methods (e.g. Lee et al. 1990; Fardin et al. 2004; Shirono and Kulatilake 1997; Kulatilake et al. 2006; Babanouri et al. 2013; Li and Huang 2015) have been proposed to quantify the joint roughness.

According to Brown (1981), the joint roughness coefficient (JRC) proposed by Barton and Choubey (1977) has been accepted by researchers and engineers all over the world in rock engineering practices. Also, it has been adopted by the ISRM Commission. It is the only quantity in Barton's empirical equation that must be estimated (Tse and Cruden 1979). Maerz et al. (1990) and Fifer-Bizjak (2010) pointed out that JRC is not a measure of the joint profile geometry, but, more properly, is an empirical parameter specifically functional to the Barton–Bandis shear strength criterion for rock joints. Although JRC cannot be used to characterize three-dimensional (3D) roughness (Grasselli et al. 2002), it is still the most commonly used parameter for quantifying joint roughness (özvan et al. 2014; Maerz et al.

Published online: 03 February 2017

1990). The tilt test (or self-weight gravity shear test) is performed on a regular basis to characterize the roughness of rock joints, and it requires transport of rock samples from the site and cutting of rock samples in the laboratory. It is difficult to collect rock joint samples of sufficient amount, and the samples are easily broken in transport or cutting (Hu and Cruden 1992). In addition, JRC evaluation by tilt test is an inverse process of shear strength analysis based on JRC-JCS model, and it is impractical to determine the rock joint roughness via a large number of tilt tests in engineering practice (Du 1994).

Barton and Choubey (1977) proposed a corresponding JRC value for ten standard profiles ranging from 0 to 20. In such methods, the JRC value of a sample can be determined by visually comparing its roughness to the standard profiles. Yet this procedure is not entirely adequate for quantifying the rock joint roughness profile in either the field or laboratory study (Beer et al. 2002; Grasselli and Egger 2003; Xia et al. 2014; Alameda-Hernández et al. 2014; Gao et al. 2015). To analyze the reliability of this traditional visual assessment method, Beer et al. (2002) performed a survey based on three granite block profiles with 125, 124, and 122 answers using an internet-based survey system. The result from a sample of ten people indicated that a wide range of JRC estimation values. Indeed, the JRC mean value and standard deviation varied significantly until the sample size exceeded 50 people. Alameda-Hernández et al. (2014) performed a similar visual estimation survey in the consideration of the knowledge and skill of the evaluators. Based on the same 12 test profiles, 74 undergraduate students showed standard deviations of JRC values ranging from 1.6 to 3.5. Nine post-graduate students showed standard deviations of 0.3–3.9, and six experts had standard deviations varying from 0.6 to 3.4. The results clearly indicated the unreliability of the JRC visual evaluating method. If the JRC values of joints are estimated inaccurately, large errors may result in the estimating of the shear strength of joints, especially when the normal stress is low.

To overcome the disadvantages of the visual comparison method, several algorithms supported by the parameters derived from digitized standard profiles have been presented for automated JRC calculations (Tse and Cruden 1979; Maerz et al. 1990; Yu and Vayssade 1991; Yang et al. 2001a, b; Tatone and Grasselli 2010; Zhang et al. 2014). Furthermore, fractal dimension values have also been reported to correlate well with JRC values (e.g. Lee et al. 1990; Huang et al. 1992; Xu et al. 2012; Jang et al. 2014; Li and Huang 2015) and numerous empirical equations were proposed for estimating JRC using fractal dimension. However, it is difficult to derive distinctive fractal dimensions for roughness profiles with self-affine characteristics and rank the suitability of these equations in engineering practice. In these quantitative assessment methods, JRC values are typically back-calculated based on a series of best-fitted roughness parameters. Although there are numbers of empirical relations between JRC values and roughness parameters with different definitions, widely accepted equations for JRC have not been established. Thus, it is necessary to develop an effective method for JRC measurement, directly using the irregularity characteristics of the standard profiles instead of curve fitting via additional roughness parameters.

Testers' subjective judgment is the major reason for assessment errors in visual comparison methods, which may be improved by introducing the similarity measures into the assessment. The effectiveness of similarity classification methods depends on how well the similarity between the standard profiles and the surface profiles for measurement is estimated. In fact, the degree of similarity or dissimilarity between the objects under study has played an important role in various scientific fields, such as pattern recognition, machine learning, decision making, and image processing (Broumi and Smarandache 2013; Majumdar and Samanta 2014; Ye 2015). In vector spaces, the Jaccard, Dice, and cosine similarity measures are often used in pattern recognition; this can effectively assess the similarity degree between the studied objects. Significantly, such vector similarity measures have not yet been applied to JRC evaluation.

In this study, the vector similarity measures were applied and profile feature vectors calculated for an objective estimation of JRC. In the vector similarity measures, the angular variations of line segments of profiles were selected to represent the irregularity characteristics of rough profiles. The feature vectors of Barton's standard profiles and test samples were obtained via inclination distribution analysis. Based on the comparisons of Jaccard, Dice, and cosine measures between the feature vectors, the JRC values of the test profiles were determined using the maximum relation index based on the similarity degree.

Preliminaries

Similarity measures are increasingly being used in various fields including data analysis and classification, pattern recognition, and decision making (Wu and Mendel 2008; Ye 2011, 2012). Vector similarity measures (VSMs) are especially useful in pattern recognition (Ye 2011). In pattern recognition and machine learning, a feature vector is a vector of numerical features that represent some object. The profile of rock joint is considered as an irregular pattern, and also can be described by the feature vector. The difference between any two profiles can be quantitatively shown by means of a similarity measure on their feature vectors. The weaknesses of existing JRC comparative

evaluation method can be eliminated by the similarity measure between the standard profiles and the test surface profiles. VSMs can be applied to JRC evaluation by obtaining and comparing the feature vectors of the irregularity characteristics from the test samples and Barton's standard profiles.

Researchers (e.g. Barton 1973; Tse and Cruden 1979; Maerz et al. 1990; Grasselli and Egger 2003) have presented roughness parameters for describing the geometric irregularities (waves) of rock joints. In addition, several algorithms of those parameters for JRC calculation have been established based on the roughness characterization analysis of the standard profiles. Among those parameters, the best results were achieved with Z_2 (Eq. 1) first-derivative root-mean-square (Tse and Cruden 1979), R_p (Eq. 2) roughness profile index or profile sinuosity (Maerz et al. 1990; Hong et al. 2008), and the roughness metric $\theta^*_{max}/(C+1)_{2D}$ proposed by Tatone and Grasselli (2010), as follows:

$$Z_2 = \sqrt{\frac{1}{L}\int_{x=0}^{x=L}\left(\frac{dy}{dx}\right)^2 dx} \approx \sqrt{\frac{1}{N}\sum_{i=1}^{N-1}\left[\frac{(y_{i+1}-y_i)}{(x_{i+1}-x_i)}\right]^2}, \quad (1)$$

$$R_p = \frac{L_t}{L_n} = \frac{\sum_{i=1}^{N-1}\sqrt{(x_{i+1}-x_i)^2+(y_{i+1}-y_i)^2}}{L_n}, \quad (2)$$

$$L_{\theta *} = L_0\left(\frac{\theta^*_{max}-\theta^*}{\theta^*_{max}}\right)^C. \quad (3)$$

where x, y are the horizontal and vertical coordinates of the points along the profile; (x_{i+1}, y_{i+1}), and (x_i, y_i) represent adjacent coordinates of the profile; N is the number of the measurements over the profile with a total length L; L_t is the true profile length and L_n is the nominal profile length; C is deduced from a regression analysis considering that $L_{\theta *}$ is the length of the fraction of the profile with a higher inclination than a threshold value θ^* divided by the total profile length; L_0 is the normalized length of the profile fraction with a positive slope and θ^*_{max}, the highest slope that appears in a fraction.

The irregularity of rock joint profiles can be reflected by an angular variation of line segments with respect to each small length (interval). If the horizontal interval between the adjacent points of the standard profiles is μ and the angle of the line segment between two adjacent points is θ_i, the formulae (1) and (2) can be rewritten as

$$Z_2 \approx \sqrt{\frac{1}{N}\sum_{i=1}^{N-1}\left(\frac{y_{i+1}-y_i}{\mu}\right)^2} = \sqrt{\frac{1}{N}}\sqrt{\sum_{i=1}^{N-1}\left(\frac{y_{i+1}-y_i}{\mu}\right)^2} = \sqrt{\frac{1}{N}}\sqrt{\sum_{i=1}^{N-1}(\tan\theta_i)^2} \quad (4)$$

$$R_p = \frac{L_t}{L_n} = \frac{\sum_{i=1}^{N-1}\sqrt{\mu^2+(y_{i+1}-y_i)^2}}{(N-1)\mu} = \frac{1}{N-1}\sum_{i=1}^{N-1}\sqrt{1+(\tan\theta_i)^2} \quad (5)$$

where

$$\tan\theta_i = \frac{y_{i+1}-y_i}{x_{i+1}-x_i} = \frac{y_{i+1}-y_i}{\mu} \quad (6)$$

As shown in formulae Z_2 (4), R_p (5), these roughness parameters largely depend on the inclination $\tan\theta_i$ of the individual lines along the profiles. In Eq. (3), the inclination θ^* of the individual line segments forming the profiles are evaluated directly. Moreover, good relationships between these related statistical parameters and JRC values have been shown in previous studies. Thus, the angular variation of line segments can be used to represent the irregularity characteristics of the profiles as the feature vector. The JRC value is determined by the similarity measures of the feature vectors of the test and standard profiles.

Let $T = (t_1, t_2, \ldots, t_n)$, and $S = (s_1, s_2, \ldots, s_n)$ be two n-dimensional vectors, which represent the feature vectors of the test object and the standard profile respectively. Then, the similarity measures between the two vectors T and S are calculated by the Jaccard similarity measure, Dice similarity measure, and cosine similarity measure.

The Jaccard index (Jaccard 1901) is defined as

$$J(T,S) = \frac{T\cdot S}{\|T\|_2^2+\|S\|_2^2-T\cdot S} = \frac{\sum_{i=1}^n t_i s_i}{\sum_{i=1}^n t_i^2+\sum_{i=1}^n s_i^2-\sum_{i=1}^n t_i s_i} \quad (7)$$

where $T\cdot S = \sum_{i=1}^n t_i s_i$ is the inner product of the vectors T and S, $\|T\|_2 = \sqrt{\sum_{i=1}^n t_i^2}$ and $\|S\|_2 = \sqrt{\sum_{i=1}^n s_i^2}$ are the Euclidean norms of T and S.

The Dice similarity measure (Dice 1945) is defined as

$$D(T,S) = \frac{2T\cdot S}{\|T\|_2^2+\|S\|_2^2} = \frac{2\sum_{i=1}^n t_i s_i}{\sum_{i=1}^n t_i^2+\sum_{i=1}^n s_i^2} \quad (8)$$

The cosine similarity measure (Salton and McGill 1987) is defined as the inner product of two vectors, which presents the cosine of the angle between two vectors. This similarity measure can be defined as follows:

$$C(T,S) = \frac{T\cdot S}{\|T\|_2\|S\|_2} = \frac{\sum_{i=1}^n t_i s_i}{\sqrt{\sum_{i=1}^n t_i^2}\sqrt{\sum_{i=1}^n s_i^2}} \quad (9)$$

These three formulae (7), (8), (9) are similar in the sense that they take values in the interval [0, 1], and $J(T, S)$, $D(T, S)$, $C(T, S)$ are equal to 1 when $T = S$.

Determination of feature vectors for the standard profiles

Feature vectors of the standard profiles are extremely important for the JRC evaluation through VSMs, which determines the accuracy of the JRC evaluation result. In order reasonably to determine the feature vector, it is necessary to study the standard profiles (Fig. 1), as introduced by Barton and Choubey (1977), separately.

In the present study, a grayscale image processing method was used for digitizing the standard profiles. Images, also known as black and white, are composed exclusively of shades of gray, varying from black at the weakest intensity to white at the strongest. The intensity of the grayscale image ranges from 0 to 255. The cells with low-intensity values in the gray matrix were highly correlated with the center line of the profile curve. The grayscale data of the imported profile images were extracted by Matlab and saved in matrix forms. Figure 2 illustrates an example of a magnified profile in the size of 1.00 mm (L) × 1.22 mm (H). It consists of 99 pixel grids, $n_x = 9$ pixels in width and $n_y = 11$ pixels in height. Then, the length μ of each pixel equals to $L/n_x = 0.11$ mm. The x_j and y_j coordinates of the center point line can be determined by $x_j = \mu(j - 1)$ and $y_j = \mu(\bar{i} - 1)$, where $j \in [1, 9]$ is the column of the grayscale matrix I, and $\bar{i}$ is the average value of the row of grayscale matrix I. By doing so, the original digitized data of both joint profiles was obtained.

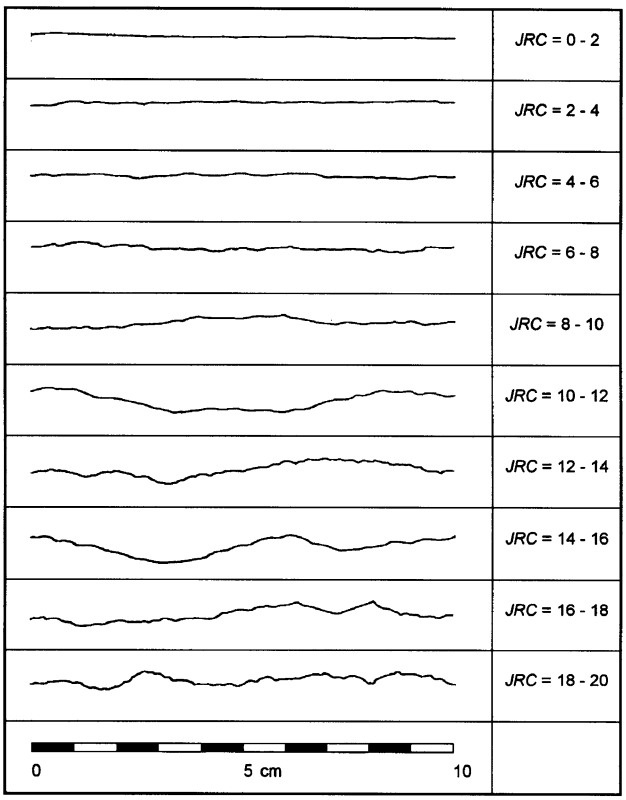

Fig. 1 Ten standard roughness profiles and corresponding JRC values by Barton and Choubey (after Hoek 2000)

The original ten images of the standard profiles by Barton and Choubey (1977) were saved in JPG format, sized in 112 × 906 pixels (profile 1), 114 × 906 pixels (profile 2), 108 × 905 pixels (profile 3), 86 × 903 pixels (profile 4), 95 × 905 pixels (profile 5), 103 × 906 pixels (profile 6), 80 × 905 pixels (profile 7), 77 × 906 pixels (profile 8), 81 × 903 pixels (profile 9), and 113 × 907 pixels (profile 10). The original image digitization ratio of these profiles was approximately 100 mm/900 ≈ 0.11 mm. In previous research, the digitization interval $\mu = 0.5$ mm was often used for analyzing roughness profiles (Yu and Vayssade 1991; Tatone and Grasselli 2010; Jang et al. 2014). In this study, ten standard profiles by Barton and Choubey (1977) were also digitized with a sampling interval of 0.5 mm, as shown in Fig. 3. Each standard profile was composed of 201 (x_i, y_i) dots. The local apparent asperity dips angle $\theta_i$of the line segment between two adjacent points along the standard profile was calculated as

$$\theta_i = \arctan\left(\sqrt{\left(\frac{y_{i+1} - y_i}{x_{i+1} - x_i}\right)^2}\right) = \arctan\left(\sqrt{\left(\frac{y_{i+1} - y_i}{\mu}\right)^2}\right) \quad (10)$$

As shown in Fig. 4, the inclination distributions of the individual line segments were plotted in histograms with a bin size of 2°. The maximum frequency counts of local apparent asperity dips were basically in 0°–2° range. The maximum value of the asperity dips in the ten standard profiles increased with the JRC value, from the minimum value 23.12° in the standard profile 1, to 48.55° in the standard profile 10. The inclination distributions of the frequency counts of the standard profiles approximately met the exponential distribution,

$$y = a \cdot \kappa^b \quad (11)$$

The frequency count κ of apparent local asperity dips with higher values increased in the standard profiles that had higher JRC values. The coefficients of exponential fitting curves of the standard profiles had corresponding variant relations with increased JRC values. Also, R-square, the coefficient of determination, decreased. For instance, the standard profile 1 had the highest frequency count value (0.61) in the range of 0° to 2°, which was more than two times larger than the standard profile 5 (0.27) and almost four times standard profile 10 (0.16). Coefficients a and b of the exponential fitting curve of standard profile 1 were 0.60 and −1.40. However, coefficient a was 0.27 and b was −0.73 in standard profile 5, and coefficient a was

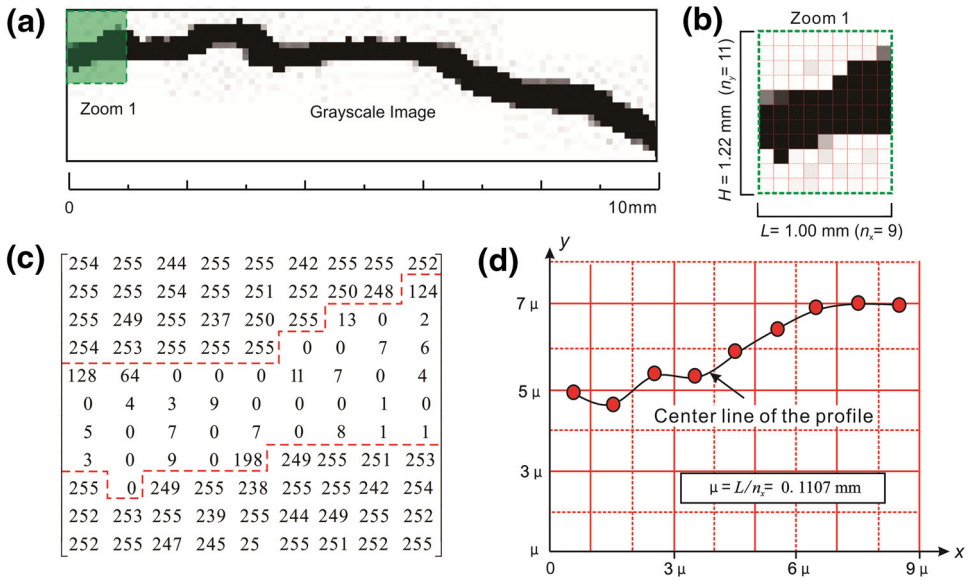

Fig. 2 Schematic diagram of principle of the joint roughness profile digitization method on the basis of image pixel analysis. **a** *Grayscale* image of the joint profile; **b** magnified zoom in 1 cm length; **c** *gray* matrix; **d** the digitized points

0.15 and b was −0.49 in standard profile 10. R-square decreased from 0.94 in standard profile 1 and to 0.66 in standard profile 10. The frequency counts of local apparent asperity dips in standard profile 10 varied from 0° to 50°, but the counts of the standard profile 1 were mainly in the range of 0°–24°. The results indicated that the ten standard profiles had distinctly different inclination distributions. Moreover, they illustrated the geometric irregularities (waves) differences between Barton's standard profiles.

The inclination distributions are presented as the feature vectors S^* with the interval of 2°. For convenient evaluation of the similarity measures, the inclination distributions were normalized by the following equation:

$$s_i = \frac{s_i^* - S_{\min}^*}{S_{\max}^* - S_{\min}^*}, \tag{12}$$

where the element s_i is the result after normalizing vector S^*, s_i^* is the count value of local apparent asperity dips in every 2 degrees, $S_{\min}^*$ and $S_{\max}^*$ are the minimum value and the maximum value of local apparent asperity dips in the vector S^*, respectively. It is important to clarify that additional local apparent asperity dips ranging between 0° and 2° may appear due to the low image accuracy of the standard profiles; these asperity dips have not been considered in the feature vector of the inclination distribution. The normalized feature vector S is tabulated in Table 1.

Similarity measures for JRC evaluation

Determination of feature vector for test profiles

The test sample profiles were obtained from natural rock joints with different surface characteristics using the mechanical hand profilograph (Du et al. 2009; Morelli 2014). The rough and irregular profiles were obtained from the bedding joints of Granite. The rough and undulating profiles were obtained from the tectonic joints of Limestone. The smooth, planar profiles were obtained from the cleavage joints of slate. These sample profiles were 10 cm long, identical to the standard profiles of Barton and Choubey (1977). The sample profiles were digitized using a similar grayscale image processing method as described in Sect. 3 for the standard profiles.

Furthermore, the inclination distributions were presented as a 15-dimensional feature vector T with the interval of 2°. For a convenient evaluation of the similarity measures, the feature vectors of the inclination distributions were expressed by the following equation:

$$t_i = \frac{t_i^* - S_{\min}^*}{S_{\max}^* - S_{\min}^*}. \tag{13}$$

For the test profiles, t_i^* represents the count value of asperity dips in every 2°. The feature vectors of the test profiles are listed in Table 2. The similarity values were obtained by similarity measures between the feature vectors S_k (1, 2,…, 10) of the standard profiles and test profiles T_j (j = 1, 2,…, 9).

JRC evaluation result

The similarity measure values of $v_k = J(S_k, T_j)$, $D(S_k, T_j)$, $C(S_k, T_j)$ (k = 1, 2, …, 10; j = 1, 2, …, 9) were obtained by Eqs. (7), (8), (9) and the range of the v_k was normalized from [0, 1] into [–1, 1] for convenient evaluation by the following relation index:

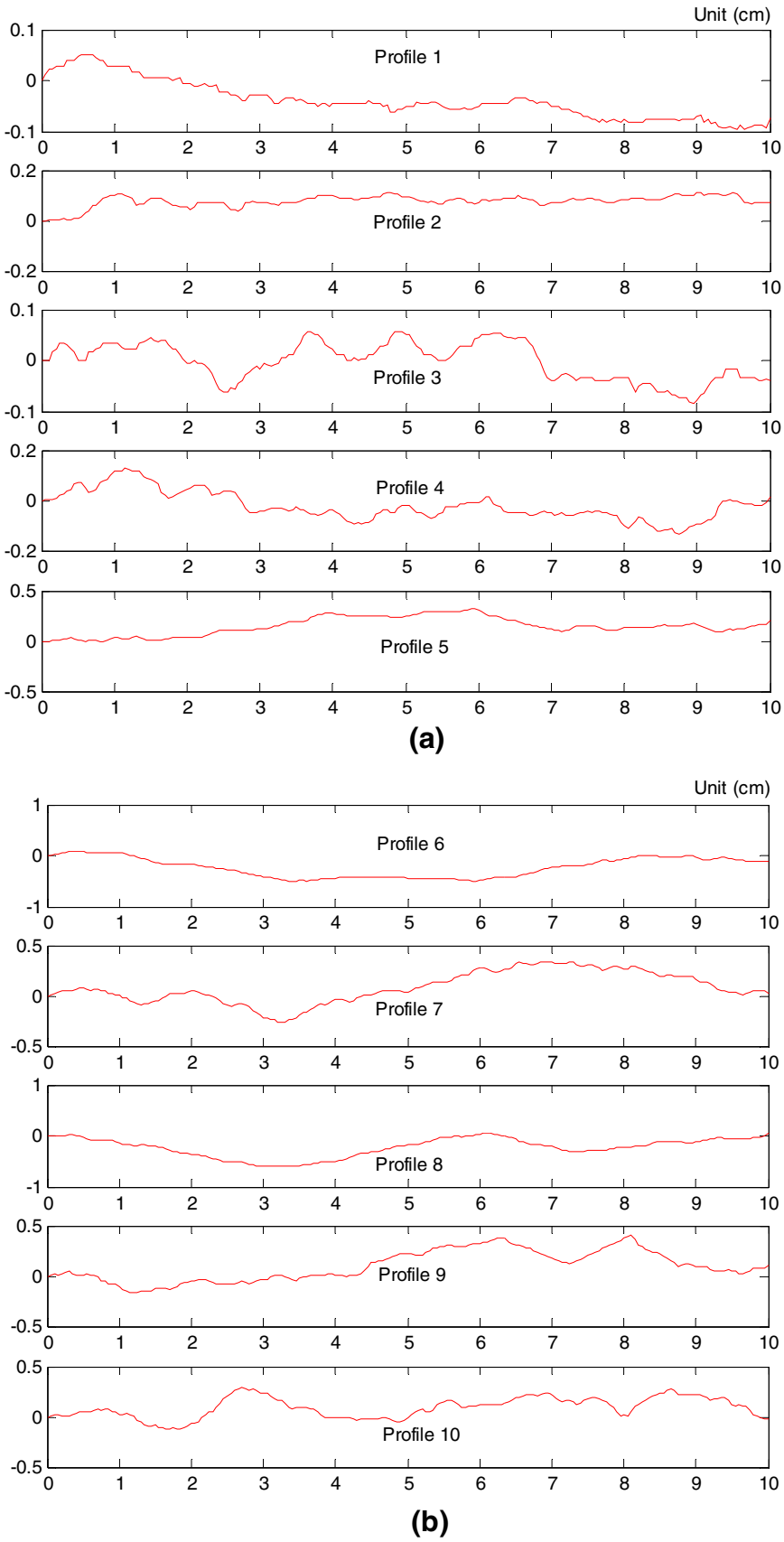

Fig. 3 Digitized standard profiles obtained by *grayscale* image processing method

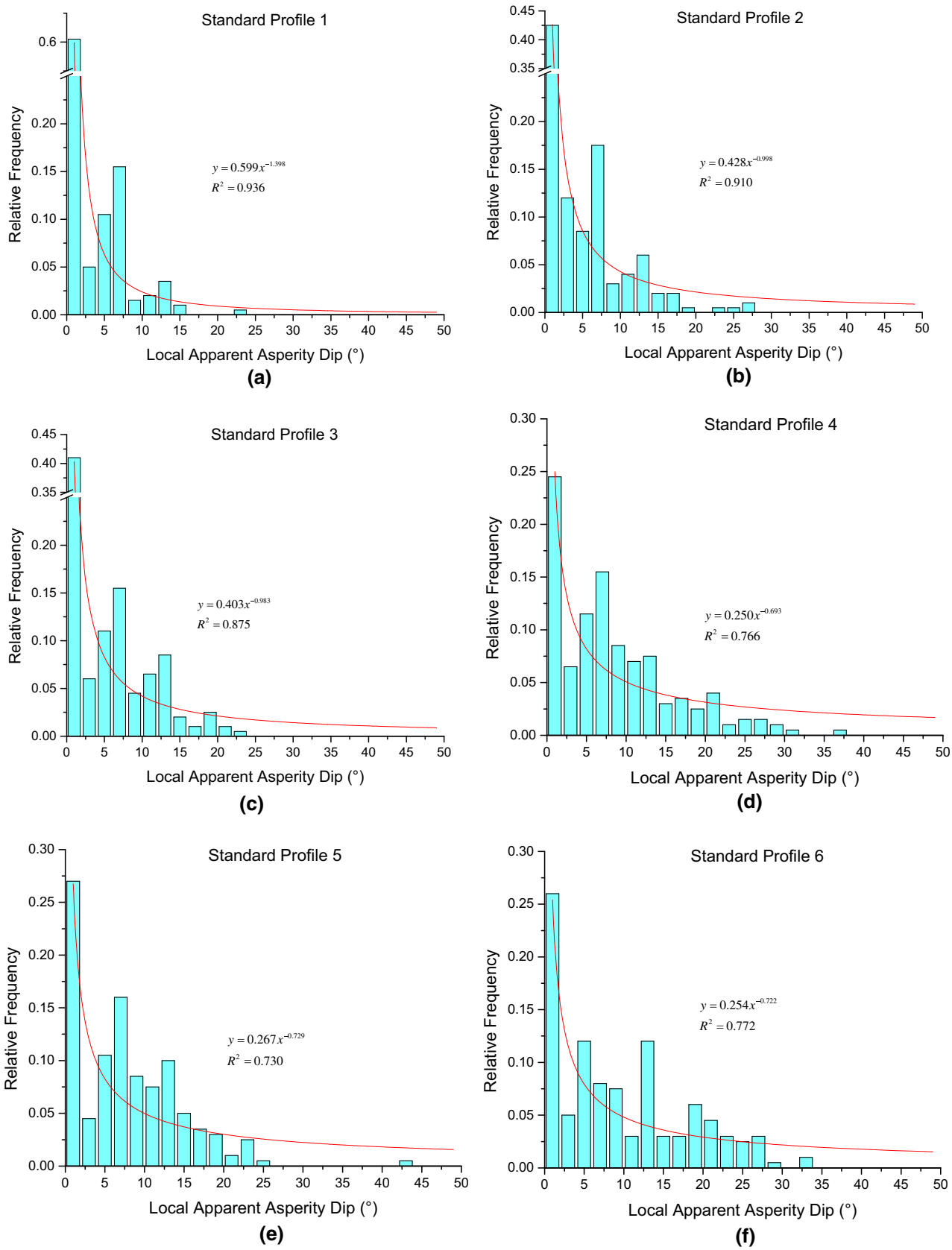

Fig. 4 Inclination distributions of the individual line segments of each standard profile

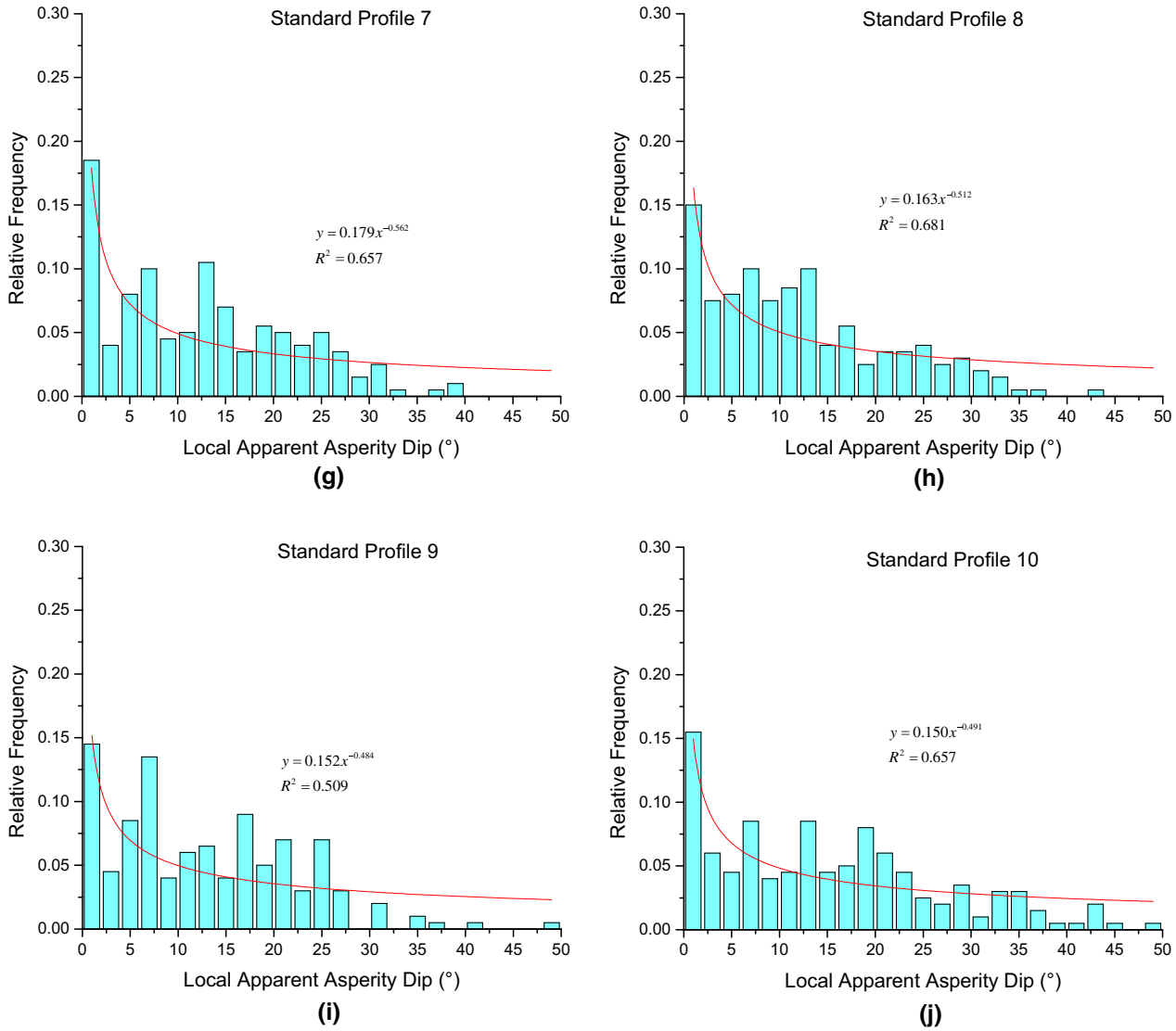

Fig. 4 continued

$$r_k = \frac{2v_k - v_{\min} - v_{\max}}{v_{\max} - v_{\min}}. \quad (14)$$

where the $v_{\max}$ and $v_{\min}$ are the maximum and minimum values of the similarity measure value v_k.

If the relation index r_k has the negative value of -1, the test profile for T_j does not have identical roughness with the k-th standard JRC profile. But, if the relation index r_k has the positive value of 1, the test profile for T_j has identical roughness with the k-th standard JRC profile. By using Eq. (14), the relation indices are shown in Table 3. The JRC values can be confirmed according to the maximum relation index. The JRC evaluation process by VSMs and relation indices is shown in Fig. 5.

For rough and irregular profiles, the JRC values of test profiles 1 and 3 are 14–16 according to the maximum relation index (1.00). This indicates that these two profiles have identical roughness with the 8th standard profile from the irregularity characteristics. The JRC value of test profile 2 is 18–20 according to the maximum relation index (1.00). This indicates that this profile has identical roughness with the 10th standard profile. The irregularity characteristics of this test profile are quite different from standard profile 1–3, and negative relation indices are obtained by VSMs method.

For rough and undulating profiles, Table 3 shows that the JRC values of profiles 4 and 6 are 10–12. This indicates that they have identical roughness with standard profile 6. The test profile 5 has a JRC value in the range of 6–8. This indicates that it has an identical roughness with standard profile 4. The JRC values of 0–2, 2–4, 12–14, 16–18,

Table 1 Normalized feature vectors of the inclination distribution for ten standard profiles

No.	JRC value	Feature vector S_k
Standard profile 1	0–2	[0.00,0.29,0.60,0.89,0.09,0.11,0.20,0.06,0.00,0.00,0.00,0.03,0.00,0.00,0.00,0.00,0.00,0.00,0.00,0.00,0.00,0.00,0.00,0.00,0.00,0.00,0.00,0.00,0.00,0.00,0.00]
Standard profile 2	2–4	[0.00,0.69,0.49,1.00,0.17,0.23,0.34,0.11,0.11,0.03,0.00,0.03,0.03,0.06,0.00,0.00,0.00,0.00,0.00,0.00,0.00,0.00,0.00,0.00,0.00,0.00,0.00,0.00,0.00,0.00,0.00]
Standard profile 3	4–6	[0.00,0.34,0.63,0.89,0.26,0.37,0.49,0.11,0.06,0.14,0.06,0.03,0.00,0.00,0.00,0.00,0.00,0.00,0.00,0.00,0.00,0.00,0.00,0.00,0.00,0.00,0.00,0.00,0.00,0.00,0.00]
Standard profile 4	6–8	[0.00,0.37,0.66,0.89,0.49,0.40,0.43,0.17,0.20,0.14,0.23,0.06,0.09,0.09,0.06,0.03,0.00,0.00,0.03,0.00,0.00,0.00,0.03,0.00,0.00,0.00,0.00,0.00,0.00,0.00,0.00]
Standard profile 5	8–10	[0.00,0.26,0.60,0.91,0.49,0.43,0.57,0.29,0.20,0.17,0.06,0.14,0.03,0.00,0.00,0.00,0.00,0.00,0.00,0.00,0.00,0.03,0.00,0.00,0.00,0.00,0.00,0.00,0.00,0.00,0.00]
Standard profile 6	10–12	[0.00,0.29,0.69,0.46,0.43,0.17,0.69,0.17,0.17,0.34,0.26,0.17,0.14,0.17,0.03,0.00,0.06,0.00,0.00,0.00,0.00,0.00,0.00,0.00,0.00,0.00,0.00,0.00,0.00,0.00,0.00]
Standard profile 7	12–14	[0.00,0.23,0.46,0.57,0.26,0.29,0.60,0.40,0.20,0.31,0.29,0.23,0.29,0.20,0.09,0.14,0.03,0.00,0.03,0.06,0.00,0.00,0.00,0.00,0.00,0.00,0.00,0.00,0.00,0.00,0.00]
Standard profile 8	14–16	[0.00,0.43,0.46,0.57,0.43,0.49,0.57,0.23,0.31,0.14,0.20,0.20,0.23,0.14,0.17,0.11,0.09,0.03,0.03,0.00,0.00,0.03,0.00,0.00,0.00,0.00,0.00,0.00,0.00,0.00,0.00]
Standard profile 9	16–18	[0.00,0.26,0.49,0.77,0.23,0.34,0.37,0.23,0.51,0.29,0.40,0.17,0.40,0.17,0.00,0.11,0.00,0.06,0.03,0.00,0.03,0.00,0.00,0.00,0.00,0.00,0.00,0.00,0.00,0.00,0.03]
Standard profile 10	18–20	[0.00,0.34,0.26,0.49,0.23,0.26,0.49,0.26,0.29,0.46,0.34,0.26,0.14,0.11,0.20,0.06,0.17,0.17,0.09,0.03,0.03,0.11,0.03,0.00,0.03]

18–20 show very low possibility due to the negative relation indices.

For smooth and even profiles, there is little difference in JRC values of test profile 7 among the results using the Jaccard similarity measure, Dice similarity measure, and cosine similarity. According to the results obtained through the cosine measure, the JRC value of this profile roughness is 4–6 according to maximum relation index (1.00), the second maximum relation is 0.95 (JRC 6–8). The maximum relation index (1.00) obtained through the Jaccard similarity measure and Dice similarity measure have identical roughness with the JRC 6–8, and the second maximum relation is 0.93 and 0.94 (JRC 4–6), respectively. The difference between the maximum and the second maximum relation index was observed to be minimal and insignificant for the overall results. This agrees with Ye (2014) who has pointed out that the Jaccard and Dice similarity measures are better than the cosine method in the similarity identification. The JRC values of test profiles 8 and 9 are 2–4 due to maximum relation index (1.00). This indicates that these profiles have identical roughness as the 2nd standard profile, and the JRC values of 8–10, 10–12, 12–14, 14–16, 16–18, and 18–20 have very low possibility due to the negative relation indices.

Comparisons with other measures for JRC

It has long been recognized that sampling interval plays an important role in obtaining accurate estimations for roughness parameters (Yu and Vayssade 1991; Yang et al. 2001a, b; Tatone and Grasselli 2010; Jang et al. 2014; Fathi et al. 2016). However, to date, there are no widely adopted methods or suggested guidelines to determine the reasonable resolution for the measurement of discontinuity roughness (Tatone and Grasselli 2013). To solve this problem, the empirical equations for estimating JRC are generally studied by a certain sampling interval. In engineering practice, the joint profiles are usually measured by the profile comb which is only capable of obtaining measurements at a certain horizontal interval between 0.5 and 1 mm. The sampling interval of 0.5 mm could indicate more detailed geometric irregularities of joint surfaces and the correlations between statistical parameters and JRC values were studied using the same sampling interval in previous literature (e.g. Yu and Vayssade 1991; Yang et al. 2001a, b; Tatone and Grasselli 2010). Therefore, a sampling interval of 0.5 mm was used in this study and the JRC values can be calculated by following equations:

$$\mathrm{JRC} = 61.79 \cdot Z_2 - 3.47, \tag{15}$$

$$\mathrm{JRC} = 32.69 + 32.98 \cdot \log_{10} Z_2, \tag{16}$$

$$\mathrm{JRC} = 51.85(Z_2)^{0.60} - 10.37. \tag{17}$$

Table 2 Normalized feature vectors of the inclination distribution of the test profiles

Test Profile NO.	Description	Digitized roughness profile (cm)	Feature vector T_j
1	Granite: rough, irregular, bedding joints	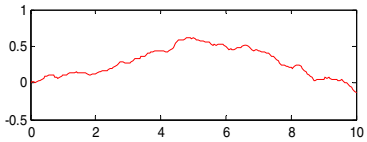	[0.00,0.23,0.29,0.31,0.49,0.54,0.29,0.26,0.34,0.29,0.34,0.26,0.09,0.11,0.11,0.09,0.03,0.09,0.06,0.00,0.00,0.00,0.03,0.00,0.00]
2	Granite: rough, irregular, bedding joints	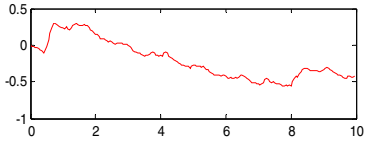	[0.00,0.09,0.17,0.20,0.60,0.17,0.06,0.20,0.60,1.43,0.17,0.11,0.23,0.17,0.11,0.09,0.06,0.03,0.00,0.03,0.03,0.03,0.06,0.00,0.03]
3	Granite: rough, irregular, bedding joints	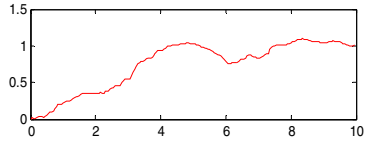	[0.00,0.40,0.49,0.20,0.54,0.94,0.06,0.31,0.17,0.34,0.09,0.23,0.09,0.11,0.06,0.11,0.03,0.09,0.06,0.00,0.00,0.03,0.00,0.03,0.03]
4	Limestone: rough, undulating, tectonic joints	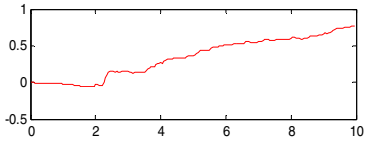	[0.00,0.26,1.00,0.09,0.60,0.54,0.17,0.17,0.09,0.11,0.06,0.03,0.03,0.06,0.06,0.03,0.03,0.00,0.03,0.00,0.00,0.00,0.00,0.00,0.06]
5	Limestone: rough, planar, tectonic joints	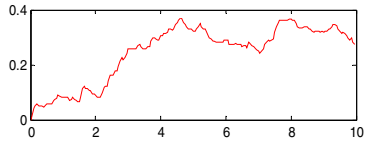	[0.00,0.34,0.74,0.26,1.37,0.14,0.20,0.03,0.29,0.14,0.09,0.03,0.09,0.00,0.03,0.00,0.03,0.00,0.00,0.00,0.00,0.00,0.00,0.00,0.00]
6	Limestone: rough, undulating, tectonic joints	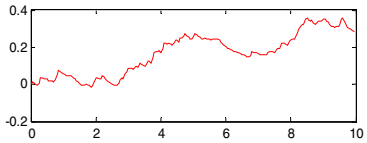	[0.00,0.26,1.00,0.09,0.60,0.54,0.17,0.17,0.09,0.11,0.06,0.03,0.03,0.06,0.06,0.03,0.03,0.00,0.03,0.00,0.00,0.00,0.00,0.00,0.06]
7	Slate: smooth, planar: cleavage joints	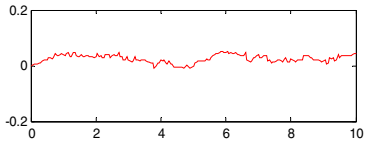	[0.00,0.31,1.51,0.37,0.20,0.63,0.20,0.11,0.11,0.03,0.06,0.03,0.03,0.00,0.00,0.00,0.00,0.00,0.00,0.00,0.00,0.00,0.00,0.00,0.00]
8	Slate: smooth, planar: cleavage joints	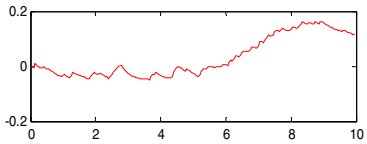	[0.00,1.91,1.03,0.54,0.34,0.11,0.26,0.09,0.00,0.03,0.03,0.00,0.00,0.00,0.00,0.00,0.00,0.00,0.00,0.00,0.00,0.00,0.00,0.00,0.00]
9	Slate: smooth, planar: cleavage joints	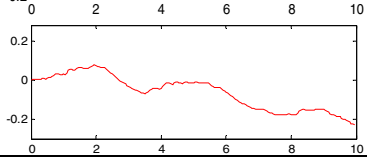	[0.00,1.57,0.83,0.97,0.40,0.06,0.09,0.03,0.00,0.00,0.00,0.00,0.00,0.00,0.00,0.00,0.00,0.00,0.00,0.00,0.00,0.00,0.00,0.00,0.00]

When sampling interval is 0.5 mm, the equation for estimating JRC from R_p is

$$\mathrm{JRC} = \left[3.36 \times 10^{-2} + \frac{1.27 \times 10^{-3}}{\ln(R_p)}\right]^{-1}. \quad (18)$$

The equation by Tatone and Grasselli (2010) to estimate JRC for sampling interval of 0.5 mm is expressed as

$$\mathrm{JRC} = 3.95(\theta^*_{\max}/[C+1]_{2D})^{0.7} - 7.98. \quad (19)$$

Table 4 presents the roughness parameters Z_2, R_p, $\theta^*_{\max}/[C+1]_{2D}$, and the results of JRC validation through the Eqs. (15)–(19). For test profile 1, the minimum JRC values and maximum value by roughness parameters are 14.26 and 15.51, respectively, which is within the JRC 14–16 range by similarity measures. For test profile 2, the JRC values obtained by Eqs. (15)–(19) are 21.96, 19.98, 20.08, 19.30, 25.40, respectively. However, according to the JRC evaluation method by Barton and Choubey (1977), the

Table 3 Results of JRC evaluation by vector similarity measures

Test (profile) no.	Method	Relation indices (r_k)										JRC diagnosis result
		JRC (0–2)	JRC (2–4)	JRC (4–6)	JRC (6–8)	JRC (8–10)	JRC (10–12)	JRC (12–14)	JRC (14–16)	JRC (16–18)	JRC (18–20)	
1	r_{Jaccard}	−1.00	−0.64	−0.15	0.40	0.27	0.41	0.70	1.00	0.58	0.87	JRC (14–16)
	r_{Dice}	−1.00	−0.55	−0.01	0.51	0.40	0.53	0.77	1.00	0.67	0.90	JRC (14–16)
	r_{cosine}	−1.00	−0.51	0.00	0.57	0.48	0.52	0.74	1.00	0.71	0.85	JRC (14–16)
2	r_{Jaccard}	−1.00	−0.73	−0.42	0.02	0.00	0.49	0.50	0.24	0.66	1.00	JRC (18–20)
	r_{Dice}	−1.00	−0.66	−0.29	0.16	0.14	0.59	0.60	0.37	0.73	1.00	JRC (18–20)
	r_{cosine}	−1.00	−0.72	−0.35	0.06	0.03	0.52	0.55	0.29	0.62	1.00	JRC (18–20)
3	r_{Jaccard}	−1.00	−0.50	0.02	0.52	0.41	0.12	0.28	1.00	0.18	0.23	JRC (14–16)
	r_{Dice}	−1.00	−0.40	0.14	0.61	0.50	0.24	0.39	1.00	0.30	0.35	JRC (14–16)
	r_{cosine}	−1.00	−0.45	0.12	0.59	0.49	0.22	0.38	1.00	0.27	0.37	JRC (14–16)
4	r_{Jaccard}	−0.83	−0.94	0.33	0.93	0.54	1.00	−0.17	0.71	−0.56	−1.00	JRC (10–12)
	r_{Dice}	−0.80	−0.93	0.40	0.94	0.59	1.00	−0.10	0.75	−0.50	−1.00	JRC (10–12)
	r_{cosine}	−0.75	−0.96	0.39	0.96	0.61	1.00	−0.11	0.74	−0.52	−1.00	JRC (10–12)
5	r_{Jaccard}	−1.00	−0.62	−0.07	1.00	0.69	0.89	−0.35	0.61	−0.31	−0.67	JRC (6–8)
	r_{Dice}	−1.00	−0.56	0.02	1.00	0.74	0.91	−0.26	0.66	−0.22	−0.62	JRC (6–8)
	r_{cosine}	−1.00	−0.73	−0.03	1.00	0.69	0.99	−0.32	0.69	−0.37	−0.65	JRC (6–8)
6	r_{Jaccard}	−1.00	−0.76	0.07	0.92	0.67	1.00	−0.25	0.52	−0.55	−0.82	JRC (10–12)
	r_{Dice}	−1.00	−0.72	0.16	0.94	0.71	1.00	−0.16	0.59	−0.49	−0.78	JRC (10–12)
	r_{cosine}	−0.97	−1.00	0.05	0.79	0.52	1.00	−0.27	0.50	−0.76	−0.85	JRC (10–12)
7	r_{Jaccard}	0.34	0.08	0.93	1.00	0.69	0.59	−0.17	0.29	−0.06	−1.00	JRC (6–8)
	r_{Dice}	0.42	0.17	0.94	1.00	0.74	0.65	−0.08	0.38	0.04	−1.00	JRC (6–8)
	r_{cosine}	0.73	0.11	1.00	0.95	0.66	0.69	−0.07	0.36	−0.05	−1.00	JRC (4–6)
8	r_{Jaccard}	−0.36	1.00	0.01	0.14	−0.33	−0.36	−0.93	−0.19	−0.85	−1.00	JRC (2–4)
	r_{Dice}	−0.28	1.00	0.10	0.24	−0.24	−0.27	−0.92	−0.09	−0.83	−1.00	JRC (2–4)
	r_{cosine}	0.11	1.00	0.13	0.09	−0.45	−0.28	−0.95	−0.13	−1.00	−0.91	JRC (2–4)
9	r_{Jaccard}	−0.03	1.00	0.09	0.18	−0.20	−0.60	−0.93	−0.37	−0.70	−1.00	JRC (2–4)
	r_{Dice}	0.10	1.00	0.22	0.30	−0.08	−0.51	−0.91	−0.25	−0.63	−1.00	JRC (2–4)
	r_{cosine}	0.43	1.00	0.22	0.17	−0.26	−0.59	−1.00	−0.33	−0.80	−1.00	JRC (2–4)

maximum JRC value should be in the range of 18–20. Thus, the suggested JRC value by similarity measures in this paper is 18–20. For the test profile 3, the JRC values based on roughness parameters are 14.51, 15.01, 14.35, 14.97, and 17.49. The JRC value of this profile roughness suggested by this paper is 14–16 due to maximum relation index (1.00). The results by Eqs. (15), (16), (17), and (18) are in the suggested range and JRC through $\theta^*_{\max}/[C+1]_{2D}$ is little higher. Because feature vectors refer to the absolute angle of the line segment between two adjacent points along the standard profile, the same part in roughness parameters Z_2, R_p. But the angle value is considered to be positive or negative in roughness parameter $\theta^*_{\max}/[C+1]_{2D}$ according to the shear directions. For test profile 4, the JRC values by roughness parameters are 9.43, 10.26, 9.88, 10.20, 9.10, which are in the value range 10–12 due to maximum relation index (1.00) by similarity measures. For test profile 5, the JRC value by similarity measures has identical roughness with the 4th standard JRC profile (6–8). The JRC values through Z_2, R_p are 7.10, 7.40, 7.60, and 8.09. The JRC values of test profile 6 are 9.68, 10.53, 10.13, 10.795, 15.62 through roughness parameters. However, the suggested JRC value of test profile 6 is between 10 and 12, which is the same as test profile 4. For test profile 7, the JRC values by roughness parameters are 4.726, 3.76, 5.06, 5.52, and 3.43, respectively. As we know, the JRC value suggested by the cosine measure is 4-6, due to maximum relation index (1.00). Therefore, the JRC values by Eqs. (15), (17) and (18) were also within this range. However, the results using the Jaccard and Dice similarity measure range between JRC 6 and JRC 8, which are higher than the values obtained by roughness parameters. Nevertheless, different methods of measurement may indicate the difference in the evaluation results. The Jaccard and Dice similarity measures imply stronger identification than the cosine measure (Ye 2014). For test profile

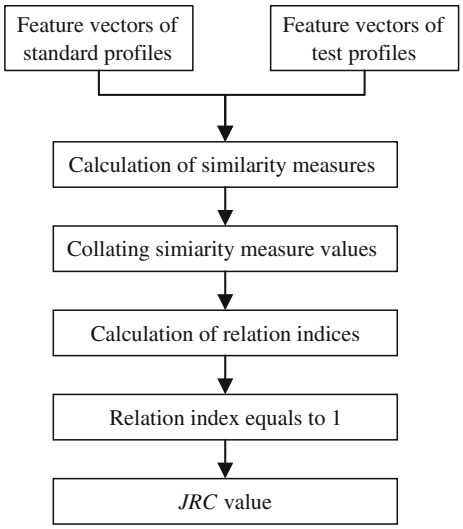

Fig. 5 Block diagram of JRC evaluation using the similarity measures of profile inclination

8, JRC values are 3.15, 0.70, 3.20, 3.88 through Z_2, R_p , and 7.483 through $\theta^*_{max}/[C+1]_{2D}$. There are obvious differences in JRC values through Z_2, which may explain JRC values even through the same roughness parameter. Moreover, the JRC value of the test profile 8 by Eq. (16) is −1.82, the solution is obviously wrong. The JRC values by Eqs. (15), (18), (19) are 2.08, 2.85, and 2.15, which are in the value range 2–4 according to maximum relation index (1.00) by similarity measures.

The JRC value is governed by how well the similarity is estimated between the standard profiles and the measured surface profile. Based on the range of JRC obtained by Eq. (14), the JRC value can be confirmed according to the relation index of two adjacent standard JRC profiles, and its value is determined by the following equation:

$$\mathrm{JRC}_k = \mathrm{JRC}^k_{\min}\left(\frac{r_{k-1}+1}{r_{k-1}+r_{k+1}+2}\right) + \mathrm{JRC}^k_{\max}\left(\frac{r_{k+1}+1}{r_{k-1}+r_{k+1}+2}\right) \tag{20}$$

where $\mathrm{JRC_k}$ is the certain value of the tested joint profile; $\mathrm{JRC^k_{min}}$ and $\mathrm{JRC^k_{max}}$ are the minimum and maximum values of k-th standard JRC profile respectively; r_{k-1} and r_{k+1} are the relation indexes of the two adjacent standard JRC profiles respectively.

Let us take the tested profile No.1 in Table as an example, and the similarity measures show that this profile well matches of $k = 8$th standard JRC profile and JRC value should be in the range of 14–16 ($\mathrm{JRC_{min}} = 14$ and $\mathrm{JRC_{max}} = 16$). Then, JRC value can be determined by how close is the test profile to 7th and 9th standard JRC profiles. If r_7 is higher than r_9, that means the JRC value is more close to the $\mathrm{JRC_{min}}$ rather than $\mathrm{JRC_{max}}$. Instead, if r_7 is lower than r_9, the JRC value should be closer to $\mathrm{JRC_{max}}$. According to the result of vector similarity measures, we can obtain the JRC values by VSMSs:

$$\begin{cases} \mathrm{JRC_{Jaccard}} = 14\left(\frac{0.70+1}{0.70+0.58+2}\right)+16\left(\frac{0.58+1}{0.70+0.58+2}\right)=14.96 \\ \mathrm{JRC_{Dice}} = 14\left(\frac{0.77+1}{0.77+0.67+2}\right)+16\left(\frac{0.67+1}{0.77+0.67+2}\right)=14.97 \\ \mathrm{JRC_{cosine}} = 14\left(\frac{0.74+1}{0.74+0.71+2}\right)+16\left(\frac{0.71+1}{0.74+0.71+2}\right)=14.99 \end{cases}$$

In addition, if the test profile is confirmed to be in the range of 0–2 or 18–20, the JRC values can be approximately estimated by using the following equation

$$\begin{cases} \mathrm{JRC}_k = \mathrm{JRC}^k_{\min} + \frac{2r_{k+1}}{1+r_{k+1}} (k=1) \\ \mathrm{JRC}_k = \mathrm{JRC}^k_{\max} - \frac{2r_{k-1}}{1+r_{k-1}} (k=10) \end{cases} \tag{21}$$

Table 4 JRC values of the test profiles calculated by Eqs. (15)–(19)

Test profile no.	Roughness parameters			JRC value				
	Z_2	R_p	$\theta^*_{max}/[C+1]_{2D}$	Through Z_2 (15)	Through Z_2 (16)	Through Z_2 (17)	Through R_p (18)	Through $\theta^*_{max}/[C+1]_{2D}$(19)
1	0.300	1.042	11.808	15.067	15.445	14.808	15.511	14.259
2	0.412	1.072	21.093	21.975	19.982	20.078	19.295	25.401
3	0.291	1.039	14.336	14.511	15.009	14.352	14.972	17.494
4	0.209	1.020	8.100	9.432	10.255	9.888	10.196	9.101
5	0.171	1.014	8.895	7.098	7.397	7.602	8.086	10.259
6	0.213	1.022	12.853	9.686	10.534	10.126	10.795	15.619
7	0.133	1.009	4.553	4.726	3.756	5.059	5.520	3.434
8	0.107	1.006	7.026	3.150	0.697	3.204	3.878	7.483
9	0.090	1.004	3.839	2.082	−1.823	1.844	2.853	2.149

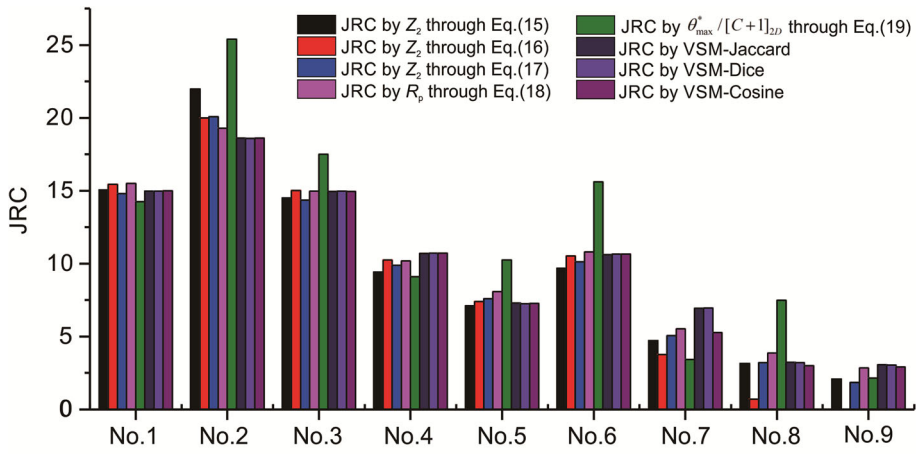

Fig. 6 JRC values of the test profiles calculated by Eqs. (15)–(19) and VSMs methods

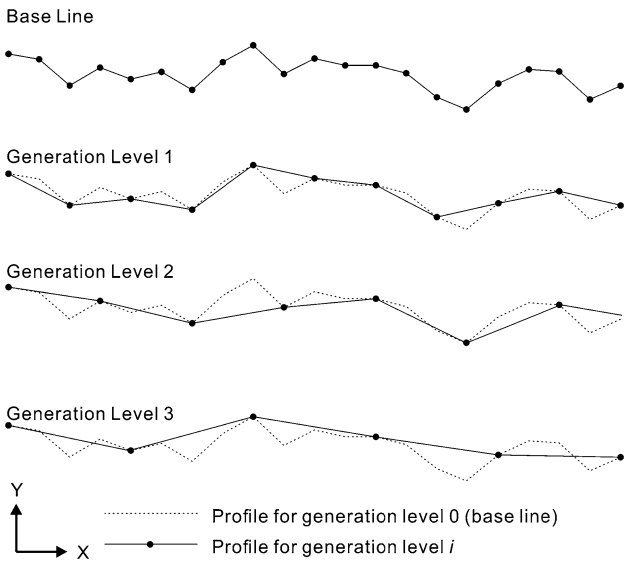

Fig. 7 Generation of the digitized profiles by various sampling intervals (after Kulatilake and Um 1999)

The distribution of the JRC values calculated via the statistical methods and VSMs are shown in Fig. 6. The predictions of JRC values from Eq. (20) agree well with the calculated values based on the relations with roughness parameters.

Discussion

The roughness profile of a natural rock joint surface is continuous, the digitized roughness profile data obtained through measurement devices are available only at a certain interval of horizontal spacing. Figure 7 shows an example of generating profiles in different resolutions, and three processed profiles generated via the random midpoint displacement method (Kulatilake and Um 1999). The profile becomes smoother under larger sampling interval, and the subprime irregular undulations between smaller horizontal spacing were neglected. Hence, the JRC values of test profiles depend on the chosen sampling interval, which means the calculated JRC values vary according to the used sampling interval.

Three different sampling intervals including 0.5, 1.5, and 2.5 mm are used to indicate the angular variation of line segments along the test joint profile No.1. The asperity dips were calculated by Eq. (10), and the frequency counts were grouped by angularly spaced dips. As shown in Fig. 8, the percentage of the asperity dips in range of 0°–10° increase with the sampling interval, but the percentage of high asperity dips reduces. By 0.5 mm sampling interval, there are 1.34% asperity dips large than 40° and 6.04% in range of 30°–40°. The percentage of asperity dips in range of 30°–40° decreases to 1.75% and no asperity dip exceeds 40° when using the sampling interval of 1.5 mm. All of asperity dips are smaller than 30° by 2.5 mm sampling interval. According to the similarity theory, the feature vectors should represent the characters of object exactly. The feature values correspond to the distributions of the asperity dips here. The distributions under 0.5 mm sampling interval show much more detailed geometric irregularities (waves) of rock joints. However, the larger sampling interval makes the feature vector less accurate.

Conclusions

JRC is one of the most important parameters utilized in calculating shear strength of rough joints in rock masses. In this study, VSMs are suggested for estimating the JRC value on the basis of the standard profiles introduced by Barton and Choubey (1977). The angular variation of line segments was used to represent the irregularity

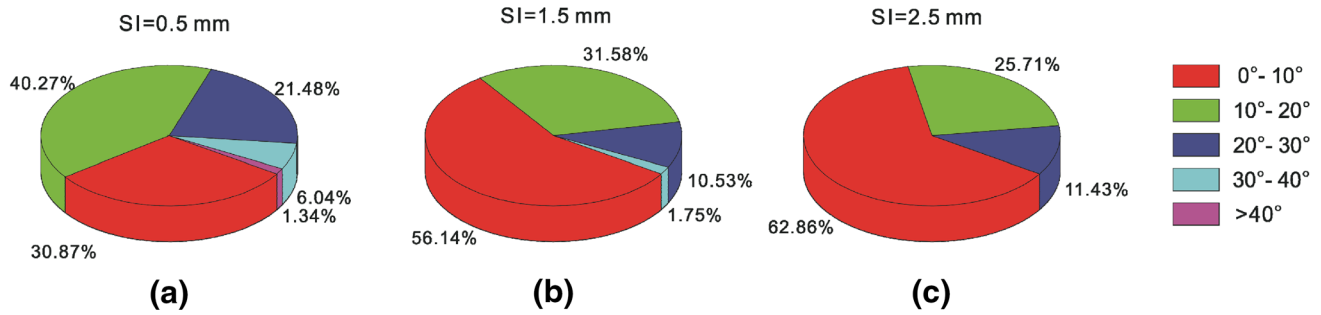

Fig. 8 *Pie chart* for the percentages of asperity dips under different sampling intervals

characteristics of the profiles as the feature vectors. The feature vectors of the standard profiles were obtained based on the profile reproducing method and inclination distribution analysis. The feature vectors of a group of nine test profiles were determined according to the undulate shapes of the ten standard profiles and test samples themselves. Additionally, we proposed the Jaccard, Dice, and cosine similarity measures between the feature vector sets of test profiles and ten standard profiles. By the calculations of the similarity measures and the relation indices, we obtained the JRC value of test profiles according to the maximum relation index (1.00). Finally, the comparative analysis was provided between the VSMs methods and the JRC evaluation methods introduced by roughness parameters of Z_2, R_p , and $\theta^*_{max}/[C+1]_{2D}$. The results of the proposed methods in this paper agreed well with previous methods. In addition, JRC evaluation methods based on VSMs were applicable and effective in the JRC evaluation. The vector similarity measure methods can overcome the drawback of the existing visual evaluation methods and indicate its rationality for JRC evaluation.

Joint surface roughness is scale dependent, so it is necessary to characterize surface roughness with multiple scales. For future work, more efforts will be made to finding a suitable VSMs for determining JRC values of different sized rock joints.

Acknowledgements The study was funded by National Natural Science Foundation of China (Nos. 41502300, 41427802, 41572299), Zhejiang Provincial Natural Science Foundation (No. Q16D020005). The authors appreciate the help provided by Harkiran Kaur, who made the careful English language editing on this manuscript before submitting. We are grateful to Prof. Ron Hotchkiss for his help with checking the data description.

References

Alameda-Hernández P, Jiménez-Perálvarez J, Palenzuela JA, El Hamdouni R, Irigaray C, Cabrerizo MA, Chacón J (2014) Improvement of the JRC calculation using different parameters obtained through a new survey method applied to rock discontinuities. Rock Mech Rock Eng 47(6):2047–2060

Andrade PS, Saraiva AA (2008) Estimating the joint roughness coefficient of discontinuities found in metamorphic rocks. Bull Eng Geol Environ 67:425–434

Babanouri N, Nasab SK, Sarafrazi S (2013) A hybrid particle swarm optimization and multi-layer perceptron algorithm for bivariate fractal analysis of rock fractures roughness. Int J Rock Mech Min Sci 60:66–74

Barton N (1973) Review of a new shear-strength criterion for rock joints. Eng Geol 7(4):287–332

Barton N (1984) Shear strength investigations for surface mining. In: 3rd International Conference on stability surface mining. Vancouver. pp 171–196

Barton N, Choubey V (1977) The shear strength of rock joints in theory and practice. Rock Mech 10(1–2):1–54

Beer AJ, Stead D, Coggan JS (2002) Technical note estimation of the joint roughness coefficient (JRC) by visual comparison. Rock Mech Rock Eng 35(1):65–74

Boutt DF, Grasselli G, Fredrich JT, Cook BK, Williams JR (2006) Trapping zones: the effect of fracture roughness on the directional anisotropy of fluid flow and colloid transport in a single fracture. Geophys Res Lett 33(21):1–6

Broumi S, Smarandache F (2013) Several similarity measures of neutrosophic sets. Neutrosophic Sets Syst 1(1):54–62

Brown ET (1981) Rock characterization testing and monitoring (ISRM suggested methods). Pergamon Press, Oxford, pp 119–183

Chen SJ, Zhu WC, Yu QL, Liu XG (2016) Characterization of anisotropy of joint surface roughness and aperture by variogram approach based on digital image processing technique. Rock Mech Rock Eng 49(3):855–876

Dice LR (1945) Measures of the amount of ecologic association between species. Ecology 26:297–302

Du S (1994) The directive statistical evaluation of rock joint roughness coefficient (JRC). J Eng Geol 2(3):62–71 **(in Chinese)**

Du S (1999) Engineering behavior of discontinuities in rock mass. Beijing: Seismological Press. pp. 1–23 (**in Chinese**)

Du S, Xu S, Yang S (2000) Application of rock quality designation (RQD) to engineering classification of rocks. J Eng Geol 8(3):351–356 **(in Chinese)**

Du S, Hu Y, Hu X (2009) Measurement of joint roughness coefficient by using profilograph and roughness ruler. J Earth Sci 20:890–896

Fardin N, Feng Q, Stephansson O (2004) Application of a new in situ 3D laser scanner to study the scale effect on the rock joint surface roughness. Int J Rock Mech Min Sci 41(2):329–335

Fathi A, Moradian Z, Rivard P, Ballivy G, Boyd AJ (2016) Geometric effect of asperities on shear mechanism of rock joints. Rock Mech Rock Eng 49(3):801–820

Fifer-Bizjak K (2010) Determining the surface roughness coefficient by 3D scanner. Geologija 53:147–152

Gao Y, Ngai L, Wong Y (2015) A modified correlation between roughness parameter Z_2 nd the JRC. Rock Mech Rock Eng 48(1):387–396

Grasselli G, Egger P (2003) Constitutive law for the shear strength of rock joints based on three-dimensional surface parameters. Int J Rock Mech Min Sci 40(1):25–40

Grasselli G, Wirth J, Egger P (2002) Quantitative three-dimensional description of a rough surface and parameter evolution with shearing. Int J Rock Mech Min Sci 39(6):789–800

Hoek E (2000) Practical rock engineering. Rock science: Course Notes and Books https://www.rocscience.com/…/Practical-Rock-Engineering-Full-Text.pdf. Accessed 01 Nov 2015

Hong ES, Lee JS, Lee IM (2008) Underestimation of roughness in rough rock joints. Int J Numer Anal Meth Geomech 32(11):1385–1403

Hu XQ, Cruden DM (1992) A portable tilting table for on-site tests of the friction angles of discontinuities in rock masses. Bull Int Assoc Eng Geol Bulletin de l'Association Internationale de Géologie de l'Ingénieur 46(1):59–62

Huang SL, Oelfke SM, Speck RC (1992) Applicability of fractal characterization and modelling to rock joint profiles. Int J Rock Mech Min Sci 29:135–153

Jaccard P (1901) Distribution de la flore alpine dans le Bassin des Drouces et dans quelques regions voisines; Bulletin de la Société Vaudoise des Sciences Naturelles. 37(140):241–272

Jang HS, Kang SS, Jang BA (2014) Determination of joint roughness coefficients using roughness parameters. Rock Mech Rock Eng 47(6):2061–2073

Kulatilake PHSW, Um J (1999) Requirements for accurate quantification of self-affine roughness using the variogram method. Int J Solids Struct 35(31):4167–4189

Kulatilake P, Balasingam P, Park J, Morgan R (2006) Natural rock joint roughness quantification through fractal techniques. Geotech Geol Eng 24(5):1181–1202

Lee YH, Carr JR, Barr DJ, Haas CJ (1990) The fractal dimension as a measure of the roughness of rock discontinuity profiles. Int J Rock Mech Min Sci 27(6):453–464

Li Y, Huang R (2015) Relationship between joint roughness coefficient and fractal dimension of rock fracture surfaces. Int J Rock Mech Min Sci 75:15–22

Maerz NH, Franklin JA, Bennett CP (1990) Joint roughness measurement using shadow profilometry. Int J Rock Mech Min Sci 27(5):329–343

Majumdar P, Samanta SK (2014) On similarity and entropy of neutrosophic sets. J Intell Fuzzy Syst 26(3):1245–1252

Morelli GL (2014) On joint roughness: measurements and use in rock mass characterization. Geotech Geol Eng 32(2):345–362

Özvan A, Dinçer İ, Acar A, Özvan B (2014) The effects of discontinuity surface roughness on the shear strength of weathered granite joints. Bull Eng Geol Environ 73:801–813

Salton G, McGill MJ (1987) Introduction to modern information retrieval. McGraw-Hill, New York

Shirono T, Kulatilake PHSW (1997) Accuracy of the spectral method in estimating fractal/spectral parameters for self-affine roughness profiles. Int J Rock Mech Min Sci 34(5):789–804

Tang H, Yong R, Eldin ME (2016) Stability analysis of stratified rock slopes with spatially variable strength parameters: the case of Qianjiangping landslide. Bull Eng Geol Environ 1–15

Tatone BSA, Grasselli G (2010) A new 2D discontinuity roughness parameter and its correlation with JRC. Int J Rock Mech Min Sci 47(8):1391–1400

Tatone BSA, Grasselli G (2013) An investigation of discontinuity roughness scale dependency using high-resolution surface measurements. Rock Mech Rock Eng 46(4):657–681

Tse R, Cruden DM (1979) Estimating joint roughness coefficients. Int J Rock Mech Min Sci 16(5):303–307

Wu D, Mendel JM (2008) A vector similarity measure for linguistic approximation: interval type-2 and type-1 fuzzy sets. Inform Sci 178(2):381–402

Xia CC, Tang ZC, Xiao WM, Song YL (2014) New peak shear strength criterion of rock joints based on quantified surface description. Rock Mech Rock Eng 47(2):387–400

Xu HF, Zhao PS, Li CF, Tong Q (2012) Predicting joint roughness coefficients using fractal dimension of rock joint profiles. Appl Mech Mater 170–173:443–448

Yang ZY, Di CC, Yen KC (2001a) The effect of asperity order on the roughness of rock joints. Int J Rock Mech Min Sci 38(5):745–752

Yang ZY, Lo SC, Di CC (2001b) Reassessing the joint roughness coefficient (JRC) estimation using Z2. Rock Mech Rock Eng 34(3):243–251

Ye J (2011) Cosine similarity measures for intuitionistic fuzzy sets and their applications. Math Comput Model 53(1):91–97

Ye J (2012) Multicriteria decision-making method using the Dice similarity measure based on the reduct intuitionistic fuzzy sets of interval-valued intuitionistic fuzzy sets. Appl Math Model 36(9):4466–4472

Ye J (2014) Vector similarity measures of hesitant fuzzy sets and their multiple attribute decision making. Econ Comput Econ Cybern Stud Res 48(4)

Ye J (2015) Improved cosine similarity measures of simplified neutrosophic sets for medical diagnoses. Artif Intell Med 63:171–179

Yong R, Hu X, Tang H, Li C, Wu Q (2013) Effect of sample preparation error on direct shear test of rock mass discontinuities. J Central South Univ (Sci Technol) 11:4645–4651 **(in Chinese)**

Yu X, Vayssade B (1991) Joint profiles and their roughness parameters. Int J Rock Mech Min Sci 28(4):333–336

Zhang GC, Karakus M, Tang HM, Ge YF, Zhang L (2014) A new method estimating the 2D joint roughness coefficient for discontinuity surfaces in rock masses. Int J Rock Mech Min Sci 72:191–198

Zhao Z, Li B, Jiang Y (2014) Effects of fracture surface roughness on macroscopic fluid flow and solute transport in fracture networks. Rock Mech Rock Eng 47:2279–2286

Zimmerman RW, Bodvarsson GS (1996) Hydraulic conductivity of rock fractures. Transp Porous Media 23(1):1–30